

A Unified Analysis of the Fault Tolerance Capability in Six-phase Induction Motor Drives

W.N.W.A. Munim^{1,4}, Mario J. Duran², Hang Seng Che¹, Mario Bermúdez³, Ignacio González-Prieto², Nasrudin Abd Rahim^{1,5}

¹UMPEDAC, University of Malaya, Kuala Lumpur, Malaysia ²University of Malaga, Malaga, Spain
³University of Seville, Seville, Spain ⁴Faculty of Electrical Engineering, Universiti Teknologi MARA (UiTM),
⁵Renewable Energy Research Group, King Abdulaziz University, Jeddah 21589, Saudi Arabia.

Abstract– The fault tolerance of electric drives is highly appreciated at industry for security and economic reasons, and the inherent redundancy of six-phase machines provides the desired fault-tolerant capability with no extra hardware. For this reason some recent research efforts have been focused on the fault-tolerant design, modelling and control of six-phase machines. Nevertheless, a unified and conclusive analysis of the post-fault capability of six-phase machine is still missing. This work provides a full picture of the post-fault derating in generic six-phase machines and a specific analysis of the fault-tolerant capability of the three mainstream six-phase induction machines (asymmetrical, symmetrical and dual three-phase). Experimental results confirm the theoretical post-fault current limits and allow concluding which is the best six-phase machine for each fault scenario and neutral arrangement.

Index Terms– Six-phase drives, fault-tolerance, field oriented control.

I. INTRODUCTION

The development of power electronics converters has popularized the use of electric drives both in autonomous systems (e.g. electric vehicles) and in industrial applications where the electric machine is decoupled from the power system (e.g. full-power wind energy systems). In such cases the number of phases is not restricted and this has encouraged researchers to reexamine the selection of the three-phase machinery as the best option [1]. It is in this scenario that multiphase machines have rejuvenated since the beginning of the 20th century [2]. During this period of reemergence, a whole new field has been tread and the know-how from three-phase drives technology has been gradually extended to cover multiphase modeling, design, modulation and control issues [3-5]. Nevertheless, the most interesting part in this progress has not been the mere extension of existing three-phase techniques, but the invention of new ways to exploit the additional degrees of freedom in multiphase machines. Some of these advantages have been recently devised (e.g. capacitor voltage balancing or charging process in electric vehicles [6,7]) whereas others were well-known prior to the survey of [1] in 2008. Among the ‘classical’ uses of the degrees of freedom, the fault tolerance provided by the redundant phases is the most appreciated feature at industry and also a widely covered topic in the literature [5].

Even though the analysis of the fault tolerance in five-phase drives has drawn attention within the scientific community [8-10], the development of multiphase demonstrators and industrial products has been mainly restricted to machines with multiple sets of three-phase

windings [11-14]. This is fundamentally due to the fact 3k-phase machines inherit the well-established three-phase technology and this reduces to some extent the uncertainty in new developments. In the high-power range, the use of multiple converters in parallel becomes mandatory, and consequently the shift to multiphase systems only implies the connection of these converters to independent sets of three-phase windings. Good examples can be found in multi-MW wind turbines [11-12], high-speed elevators [13] and aircraft systems [14], equipped with multiple three-phase back-to-back modules that feed a 3k-phase machine. Another reason to use machines with multiple three-phase windings is the need for a lower input voltage, as it is the case in GaN-based power switches [15].

Regardless of the motivation to use a 3k-phase machine, the existence of multiple (redundant) windings opens the possibility to withstand open-circuit faults (OCFs) with no extra hardware and a smooth post-fault operation. The post-fault capability is however dependent on the arrangement of the supplying voltage source converters (VSCs). If the dc-links are cascaded, the fault tolerance is lost unless one uses parallel converters [6,16] and if the dc-links are independent then the OCFs imply the disconnection of the whole three-phase VSC [11,12]. The fault tolerance can however be improved by using a single dc-link because the power oscillations of the faulted VSC can be compensated by the healthy ones obtaining a constant dc-link power [17,18].

It is noted that the OCFs can occur as either open IGBT fault or open-phase fault (OPF). The former case refers to the condition where one or more IGBT(s) in a converter leg is open circuited, due to either IGBT gating failure [9] or fault remedial control (e.g. for the one-transistor trigger suppression control in [19]), such that the antiparallel diode(s) is still functional. On the other hand, OPF refers to the case where one or more phase connection(s) between the converter and machine is completely open-circuited, due to poor connection issues [20] or fault remedial actions that disconnect the phase using protection devices such as circuit breakers or fuses [21]. While the two cases represent significantly different OCFs, it has been demonstrated in [9] that standard post-fault strategy based on OPF gives satisfactory performance even during open IGBT faults (if the two switches in the same leg are kept open but the freewheeling diodes are operational). Furthermore, an open IGBT fault can be converted into an OPF using additional protection devices, which can help to reduce deterioration of the drive during post-fault operation [9]. Hence in this paper, the OCF considered is referring to the OPF.

In spite of the interest on the fault-tolerance of six-phase machines in single dc-link configuration, the simple question ‘Which is the best six-phase machine from the fault tolerance point of view?’ still lacks a conclusive answer. Traditionally, asymmetrical six-phase machine (abbreviated A6 in what follows) has been favored over the other six-phase machines for its low torque ripples when operated with six-step inverter [22]. However, with the modern high frequency pulse-width modulation (PWM) method, it has been shown that symmetrical six-phase machines can have similar torque performance as asymmetrical six-phase machines [23]. Thus, symmetrical six-phase and dual three-phase machines (abbreviated S6 and D3 in what follows, respectively) can be considered as two promising alternatives to the asymmetrical six-phase machines [24]. While the research focus has been placed mainly on the fault tolerant design [25-29], modelling [30,31] and control aspects [8-10, 32-34], there is no comparative analysis of the fault tolerant capability of these three mainstream six-phase machines.

In order to preserve the integrity of the system, a mandatory derating of the system needs to be set after the fault occurrence [35]. It has been quantified in [17] for asymmetrical six-phase machines (A6), achieving a maximum current production of 69.4% and 57.5% in single and two neutral arrangements, respectively. However, the post-fault current/torque capability of symmetrical six-phase machines (S6) and dual three-phase machines (D3) has not been stated yet. Furthermore, a unified analysis to include different winding displacements, neutral connections, modes of operation and fault scenarios is still missing. This work aims to fill this gap and provide a complete picture of the fault tolerant capability for six-phase induction machines under different arrangements and circumstances. The theoretical analysis and the subsequent experimental results allow concluding which is the best choice in terms of fault tolerance when selecting a six-phase machine.

The paper is structured as follows. Section II describes how to reconfigure the system after the fault occurrence to preserve the drive ratings. Section III uses the previously described optimization procedure to determine the current/torque derating under all independent OCF scenarios, considering different neutral connections and modes of operation. Section IV briefly describes the post-fault control strategy and section V compares the theoretical and experimental results using two different test rigs for asymmetrical, symmetrical and dual three-phase machines. The main conclusions are finally summarized in section VI.

II. OPTIMIZATION OF POST-FAULT CURRENTS

This section describes the healthy and faulted operation of six-phase drives and the optimization procedure to achieve an undisturbed fault-tolerant operation.

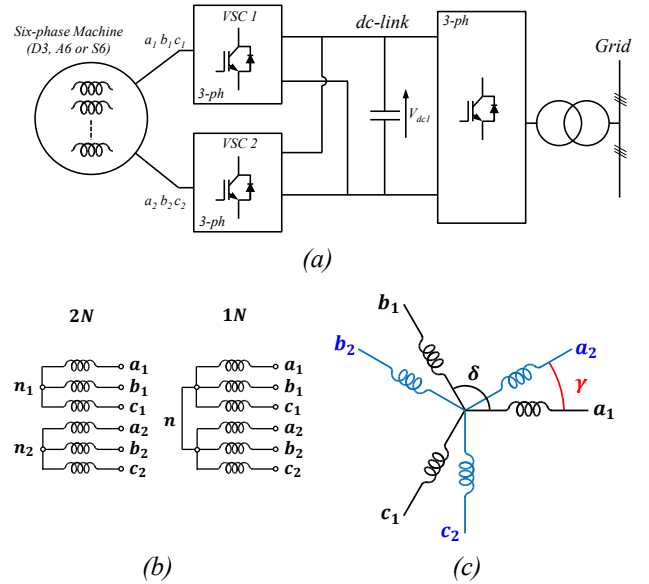


Fig. 1: a) Six-phase drive topology, b) single and two neutrals connection and c) six-phase induction motor with a generic spatial shifting γ between three-phase windings.

A. Generalities of six-phase drives

The six-phase drive under study consists of a six-phase induction motor with two sets of three-phase windings ($a_1b_1c_1$ and $a_2b_2c_2$) independently supplied by two IGBT-based two-level voltage source converters (VSC₁ and VSC₂) that are connected in parallel to a single dc-link (Fig. 1a). Three-phase windings 1 and 2 are star-connected (Fig 1b) and neutrals n_1 and n_2 can be either isolated, resulting in a two neutrals configuration (abbreviated as 2N in what follows), or connected in single neutral arrangement (abbreviated as 1N in what follows). For the sake of generality, the three-phase windings 1 and 2 are considered to be spatially shifted an arbitrary angle γ (Fig. 1c). The three mainstream six-phase machines are then specific cases of this generic machine (Fig. 2):

- D3: Dual three-phase machine ($\gamma=0^\circ$)
- A6: Asymmetrical six-phase machine ($\gamma=30^\circ$)
- S6: Symmetrical six-phase machine ($\gamma=60^\circ$)

The six-phase machine of Fig. 1c is fed with phase currents $i_{a1}, i_{b1}, i_{c1}, i_{a2}, i_{b2}, i_{c2}$ that in steady-state can be generally expressed in the time domain as:

$$\begin{aligned}
 i_{a1}(t) &= \sqrt{2} \cdot I_{a1} \cdot \cos(\omega \cdot t + \varphi_{a1}) \\
 i_{b1}(t) &= \sqrt{2} \cdot I_{b1} \cdot \cos(\omega \cdot t + \varphi_{b1}) \\
 i_{c1}(t) &= \sqrt{2} \cdot I_{c1} \cdot \cos(\omega \cdot t + \varphi_{c1}) \\
 i_{a2}(t) &= \sqrt{2} \cdot I_{a2} \cdot \cos(\omega \cdot t + \varphi_{a2}) \\
 i_{b2}(t) &= \sqrt{2} \cdot I_{b2} \cdot \cos(\omega \cdot t + \varphi_{b2}) \\
 i_{c2}(t) &= \sqrt{2} \cdot I_{c2} \cdot \cos(\omega \cdot t + \varphi_{c2})
 \end{aligned} \tag{1}$$

and can also be written as phasors in the form $I_{a1} \angle \varphi_{a1}$, $I_{a2} \angle \varphi_{a2}$, $I_{b1} \angle \varphi_{b1}$, $I_{b2} \angle \varphi_{b2}$, $I_{c1} \angle \varphi_{c1}$, and $I_{c2} \angle \varphi_{c2}$.

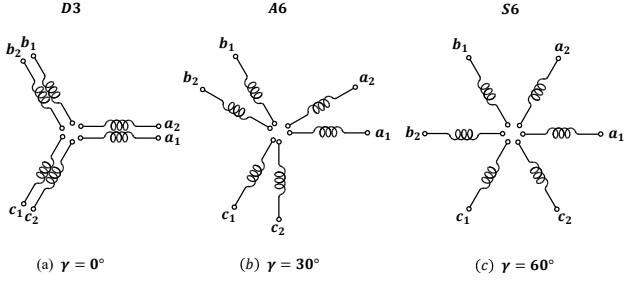


Fig. 2: Three mainstream six-phase machines: a) D3: Dual three-phase machine ($\gamma = 0^\circ$), b) A6: asymmetrical six-phase machine ($\gamma = 30^\circ$) and c) S6: symmetrical six-phase machines ($\gamma = 60^\circ$).

For convenience, phase currents can be mapped into α , β , x , y , θ_+ and θ_- components using the vector space decomposition (VSD) approach and the generalized Clarke transformation matrix:

$$[T_6] = \frac{1}{\sqrt{3}} \begin{bmatrix} 1 & \cos(\theta) & \cos(2\theta) & \cos(\gamma) & \cos(\theta + \gamma) & \cos(2\theta + \gamma) \\ 0 & \sin(\theta) & \sin(2\theta) & \sin(\gamma) & \sin(\theta + \gamma) & \sin(2\theta + \gamma) \\ 1 & \cos(2\theta) & \cos(\theta) & -\cos(\gamma) & -\cos(\theta + \gamma) & -\cos(2\theta + \gamma) \\ 0 & \sin(2\theta) & \sin(\theta) & \sin(\gamma) & \sin(\theta + \gamma) & \sin(2\theta + \gamma) \\ 1 & 1 & 1 & 0 & 0 & 0 \\ 0 & 0 & 0 & 1 & 1 & 1 \end{bmatrix} \quad (2)$$

where $\theta = 2\pi/3$.

The α - β currents are solely responsible for the flux and torque production in distributed-winding machines, whereas the x - y currents are not involved in the energy conversion process. Zero sequence currents θ_+ and θ_- can flow in 1N but they are zero in 2N. Applying Clarke matrix (2) to steady-state phase currents in (1) provides the VSD phasors $I_\alpha \angle \varphi_\alpha$, $I_\beta \angle \varphi_\beta$, $I_x \angle \varphi_x$, $I_y \angle \varphi_y$, $I_{0+} \angle \varphi_{0+}$ and $I_{0-} \angle \varphi_{0-}$.

B. Healthy operation

In healthy operation steady-state phase currents form a balanced set with equal peak values (i.e. $I_{a1} = I_{b1} = I_{c1} = I_{a2} = I_{b2} = I_{c2}$, $\varphi_{a1} = 0$, $\varphi_{b1} = \theta$, $\varphi_{c1} = 2\theta$, $\varphi_{a2} = \gamma$, $\varphi_{b2} = \theta + \gamma$, $\varphi_{c2} = 2\theta + \gamma$). In this pre-fault scenario the x - y currents are null and the α - β current phasor describes a circle in order to generate a rotating MMF that smoothly drives the machine with constant torque. This circular-shaped rotating phasor can be obtained with the conditions:

$$\begin{aligned} I_\alpha &= I_\beta \\ \varphi_\alpha &= \varphi_\beta - \pi/2 \end{aligned} \quad (3)$$

If the machine is connected with two neutrals the zero sequence current cannot flow:

$$\begin{aligned} i_{0+} &= 0 = i_{a1}(t) + i_{b1}(t) + i_{c1}(t) \\ i_{0-} &= 0 = i_{a2}(t) + i_{b2}(t) + i_{c2}(t) \end{aligned} \quad (4)$$

Alternatively, if a single neutral is used then the zero sequence current can flow from winding 1 to winding 2 or vice versa:

$$i_{0+} + i_{0-} = 0 \quad (5)$$

Apart from the neutral conditions (4)-(5), the integrity of the system is preserved by keeping phase currents below the rms rated value, i.e. $I^{pre-fault} \leq I_N$.

C. Post-fault operation

The OCFs impose new restrictions associated to the faulted phases:

$$I_k = 0 \quad \forall k \in \{\text{Faulted phases}\} \quad (6)$$

but the aim of the fault-tolerant control is to maintain the pre-fault torque with no additional torque ripple. For multiphase machine with distributed windings, this can be simply achieved if condition (3) is preserved, since the torque is maintained in post-fault situation if the fundamental MMF is kept undisturbed. The neutral restrictions (4)-(5) also apply in fault tolerant operation for 2N and 1N, respectively.

The key issue in the system reconfiguration is thus to define new current references that comply with restrictions (3)-(6), but the solution is not unique. Since the number of unknowns is higher than the number of restrictions the problem is undetermined, and consequently there is room to optimize the post-fault currents. The two most common optimization criteria used in literature lead to different modes of operation:

- Minimum loss (ML) mode. The target is to minimize the copper losses defined by the cost function J_{ML} :

$$J_{ML} = \min\{i_\alpha^2 + i_\beta^2 + i_x^2 + i_y^2 + i_{0+}^2 + i_{0-}^2\} \quad (7)$$

This mode however leads to unequal phase currents and the torque is not maximized if all phase currents are limited by $I^{post-fault} \leq I_N$.

- Maximum torque (MT) mode. In this case the cost function J_{MT} directly aims to maximize the torque, which in turn implies maximizing the amplitude of the α - β phasor:

$$J_{MT} = \max(|I_{\alpha\beta}|) \quad (8)$$

The mode of operation defines the optimization target, but it is still necessary to define the post-fault current limits. Since the machine is driven with less active phases due to the OCFs, it is in principle possible to allow overcurrents in the healthy phases but maintain the pre-fault copper losses [35,36]. This procedure may lead however to hotspots in some parts of the machine and consequently it is a common procedure to keep currents below rated values to be on the security side [5]:

$$I_k \leq I_n \quad \forall k \in \{\text{Healthy phases}\} \quad (9)$$

Once the conditions for a smooth and secure fault-tolerant operation have been set in (3)-(9), the next step is to define the optimization procedure.

D. Optimization

A first approach for the post-fault current optimization is based on phase variables. The objective of the optimization process is then to determine the twelve unknowns I_{a1} , I_{b1} , I_{c1} , I_{a2} , I_{b2} , I_{c2} , φ_{a1} , φ_{b1} , φ_{c1} , φ_{a2} , φ_{b2} , φ_{c2} from (1) that maximize the electrical torque (8) or minimize the copper losses (7) providing a rotating MMF (3) without violating the thermal limits (9) and complying with neutral (4)-(5) and fault conditions (6). The optimization problem can be summarized as:

$$\begin{aligned} \max_{(I_{a1}, I_{b1}, I_{c1}, I_{a2}, I_{b2}, I_{c2}, \varphi_{a1}, \varphi_{b1}, \varphi_{c1}, \varphi_{a2}, \varphi_{b2}, \varphi_{c2})} J_{MT} \quad \text{or} \\ \min_{(I_{a1}, I_{b1}, I_{c1}, I_{a2}, I_{b2}, I_{c2}, \varphi_{a1}, \varphi_{b1}, \varphi_{c1}, \varphi_{a2}, \varphi_{b2}, \varphi_{c2})} J_{ML} \end{aligned}$$

Subject to:

- $I_\alpha = I_\beta$
- $\varphi_\alpha = \varphi_\beta - \pi/2$
- $I_\alpha \angle \varphi_\alpha = \sqrt{2} \cdot (I_{a1} \angle \varphi_{a1} + \cos(\alpha) \cdot I_{b1} \angle \varphi_{b1} + \cos(2\alpha) \cdot I_{c1} \angle \varphi_{c1} + \cos(\gamma) \cdot I_{a2} \angle \varphi_{a2} + \cos(\alpha + \gamma) \cdot I_{b2} \angle \varphi_{b2}) + \cos(2\alpha + \gamma) \cdot I_{c2} \angle \varphi_{c2}$
- $I_\beta \angle \varphi_\beta = \sqrt{2} \cdot (\sin(\alpha) \cdot I_{b1} \angle \varphi_{b1} + \sin(2\alpha) \cdot I_{c1} \angle \varphi_{c1} + \sin(\gamma) \cdot I_{a2} \angle \varphi_{a2} + \sin(\alpha + \gamma) \cdot I_{b2} \angle \varphi_{b2} + \sin(2\alpha + \gamma) \cdot I_{c2} \angle \varphi_{c2})$
- $I_k = 0 \forall k \in \{\text{Faulted phases}\}$
- $I_k \leq I_n \forall k \in \{\text{Healthy phases}\}$
- Kirchhoff restrictions (equations (4) or (5))

(10)

that can be solved using the CONOPT optimization method included in the GAMS software [33,34,37]. However, CONOPT does not guarantee a global optimum solution, so several seeds have been used to avoid local maxima. Optimal phase currents obtained from (10) are however not suitable for control purposes because the current regulation is performed in VSD variables. Since α - β currents remain unchanged after the fault, the current reconfiguration must be performed by modifying the x - y and θ_+ - θ_- references. Consequently, it is necessary to derive the relationship between the x - y - θ_+ - θ_- and α - β currents from the phase variable results obtained from (10).

For the sake of verification, an alternative optimization method that is directly based on the VSD, similar to that in [24], is also developed. In this alternative approach, the x - y - θ_+ - θ_- are expressed in terms of the α - β currents references as:

$$\begin{aligned} i_x^* &= K_1 \cdot i_\alpha^* + K_2 \cdot i_\beta^* \\ i_y^* &= K_3 \cdot i_\alpha^* + K_4 \cdot i_\beta^* \\ i_{0+}^* &= K_5 \cdot i_\alpha^* + K_6 \cdot i_\beta^* \\ i_{0-}^* &= K_7 \cdot i_\alpha^* + K_8 \cdot i_\beta^* \end{aligned} \quad (11)$$

By optimizing the coefficients, K_1, K_2, \dots, K_8 , based on different optimization objective (minimum losses or maximum torque) the x - y and θ_+ - θ_- currents references for the corresponding post-fault modes can be attained.

While different optimization methods/software can be used for this purpose, this is done using ‘Solver’, a nonlinear optimization algorithm available as add-in in MS Office Excel. At each iteration, the coefficients will be varied, and the subsequent phase currents amplitudes are obtained by applying $[T_6]^{-1}$ onto the VSD currents. The optimization targets for minimum loss and maximum torque modes are based on (7) and (8) respectively, and are subjected to the same restrictions as in (10).

It must be noted that both approaches yield the same results for all scenarios that will be considered next to evaluate the derating of the six-phase drive.

III. DETERMINATION OF THE POST-FAULT PERFORMANCE IN SIX-PHASE DRIVES

This section examines the post-fault performance of six-phase induction motor drives considering up to three simultaneous open-circuit faults (see Fig. 3). Although the

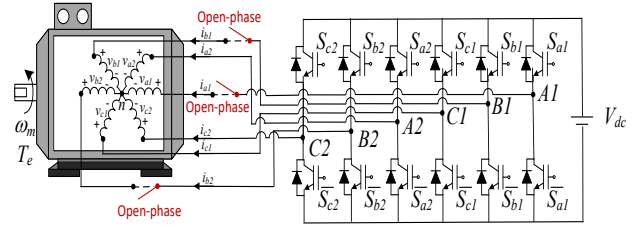


Fig. 3: Six-phase induction motor drive with open-circuit faults in phases a_1, b_1 and b_2 . One OCF in phase a_1 corresponds to scenario 1, two OCFs in phases a_1 - b_1 correspond to scenario 2a and three OCFs in a_1 - b_1 - b_2 correspond to scenario 3d shown in Table I.

faults are schematically indicated in the figure as open-phases [5], [8-10], [17-21], [28-30], [33], they correspond in general to machine faults, poor connection between the machine and the converter or IGBT faults that are subsequently converted into open-phase faults by proper isolation after the fault detection. In principle there are 41 different fault scenarios for arbitrary values of γ , but only a maximum of nine, seven and three independent fault scenarios remain for A6, S6 and D3 machines, respectively. These independent scenarios are shown as shaded boxes in Table I. The winding configurations under various fault scenarios are further illustrated in the Appendix, using an asymmetrical six-phase machine winding as example.

The reductions in number of independent fault scenarios are due to two distinctively different reasons: structural symmetry and single-phase operation. In the ‘‘structural symmetry’’ cases, the post-fault machines in two or more fault scenarios have similar post-fault structure. This gives rise to the same post-fault current waveforms (but different phase order), same derating factor and are hence considered redundant. For example, case 2d for S6 is redundant scenario for case 2b, as indicated in Table I. Apart from structural symmetry, there are scenarios where α and/or β currents are no longer controllable, making condition (3) impossible. In such scenarios, the machine is reduced to be equivalent to a single-phase machine, and post-fault operation is not possible. Such single-phase operation scenarios are indicated as ‘‘-’’ in Table I.

To facilitate further discussion, several important performance indicators are first explained here:

- **The derating factor (a):** It is the per unit value of the post-fault α - β current phasor modulus, with restriction that the maximum post-fault phase current does not exceed the rated phase current [17]. This is in accordance with (9) and keeps the drive on the safe side against thermal overheating and hot spots [5] at the expense of post-fault α - β current phasor modulus below rated values. For example, in S6 the post-fault modulus α - β is 1.888751 while the rated modulus α - β is 2.4495. Therefore the derating factor as in (12) gives 0.771.

$$a = \frac{|I_{\alpha\beta}|_{\text{Post-fault}}}{|I_{\alpha\beta}|_{\text{Rated}}} \quad (12)$$

This is the most insightful performance indicator since the post-fault current and torque production is proportional to a and a^2 , respectively in induction

machine (both current and torque would be proportional to a in PMSMs). It is worth noted that the derating factor does not depend on the machine parameters.

- **The neutral factor (k_N):** It is the improvement of the derating factor a when the machine is configured with single neutral (1N) compared to the two neutrals (2N).

$$k_N = \frac{a_{1N} - a_{2N}}{a_{2N}} \times 100 \quad (13)$$

- **The mode of operation factor (k_M):** It is the improvement of the derating factor a with maximum torque (MT) compared to minimum loss (ML) criterion:

$$k_M = \frac{a_{MT} - a_{ML}}{a_{ML}} \times 100 \quad (14)$$

Performance indicators (12)-(14) are shown in Fig. 4-6 for the scenarios indicated in Table I. The format of the legends in all figures includes the neutral connection (1N or 2N), an hyphen and the fault scenario (1, 2a, 2b, 2c, 2d, 3a, 3b, 3c, 3d). For symmetry considerations, the shifting between windings γ is only varied from 0 to 60°.

Optimizations based on section II-D are implemented onto the fault scenarios, and the corresponding performances indicators are obtained and shown in Fig. 4-6.

A. Single OCF (scenario 1)

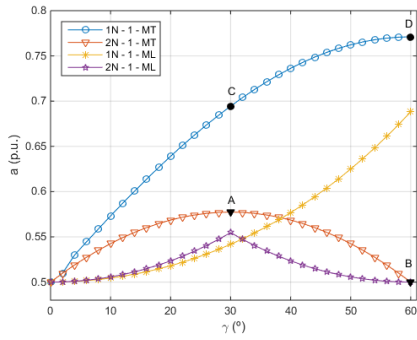
The scenario with a single OCF is firstly considered in Fig. 4. It can be noted that the D3 ($\gamma = 0^\circ$) only achieves

50% of the rated current either with single or two neutrals, resulting in a null neutral factor k_N . Since the configuration with two neutrals presents advantages in terms of dc-bus utilization and simpler control structure [24], it becomes apparent that no advantage is obtained by connecting the two neutrals. Consequently, the D3 can only operate in ‘single VSC’ mode of operation with a limited post-fault torque production of 25% the rated value.

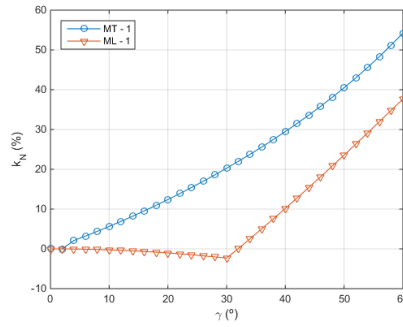
When the spatial shifting γ increases up to 30°, the derating factor increases for 2N configuration and MT criterion up to 0.577 (point A in Fig. 4a), but it decreases down to 0.5 when γ is further increase up to 60° (point B in Fig. 4a). Consequently, A6 is the best option in terms of fault tolerance if 2N is preferred. The 2N choice can still

TABLE I
INDEPENDENT FAULT SCENARIOS FOR SIX-PHASE MACHINES:
ASYMMETRICAL (A6), SYMMETRICAL (S6) AND DUAL THREE-PHASE (D3)

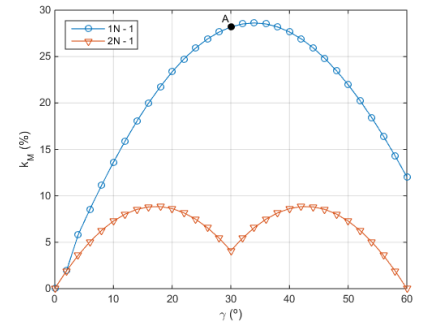
No.OCF	Scenario	Faulty ph.	A6	S6	D3
1 OCF	1	a_1			
2 OCFs	2a	a_1-b_1			
	2b	a_1-a_2			-
	2c	a_1-b_2			(2a)
	2d	a_1-c_2		(2b)	(2a)
3 OCFs	3a	$a_1-b_1-c_1$			
	3b	$a_1-b_1-a_2$			-
	3c	$a_1-b_1-c_2$			(3a)
	3d	$a_1-b_1-b_2$		(3c)	-



(a)

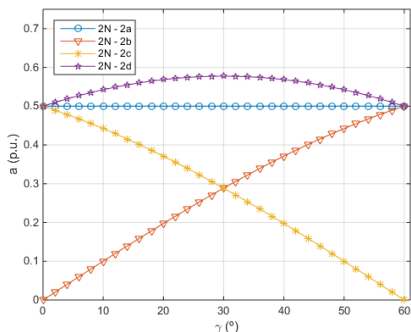


(b)

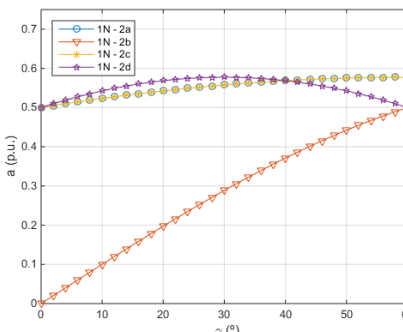


(c)

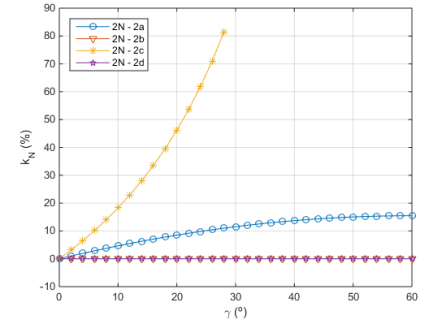
Fig. 4: a) Derating factor a versus γ for 1 OCF in single neutral (1N) and two neutrals (2N) configuration, b) Neutrals configuration factor k_N versus γ for 1 OCF using MT (blue trace) and ML (red trace) and c) Mode of operation factor k_M versus γ for 1 OCF using 1N (blue trace) and 2N (red trace).



(a)



(b)



(c)

Fig. 5: a) Derating factor a versus γ for 2 OCFs (scenarios 2a, 2b, 2c and 2d) in two neutrals (2N) configuration, b) Derating factor a versus γ for 2 OCFs in single neutral (1N) configuration and c) Neutral factor k_N versus γ for 2 OCFs using MT criterion.

preserve simplicity and good dc-bus utilization, but the post-fault torque capability is still only one third of the rated value (i.e. $a^2 = 0.577^2 = 0.33$).

The 1N connection however provides a better post-fault prospect, elevating the derating factor up to 0.694 and 0.771 for A6 and S6 using MT criterion, respectively (points C and D in Fig. 4a). Conversely, the best choice in 1N connection is the S6. While the neutral factor is 20.3% for $\gamma = 30^\circ$ (A6) using MT criterion, this value is elevated up to 54.2% for $\gamma = 60^\circ$ (S6), as seen in Fig. 4b. As a result, the torque production at point D is 23.4% higher than the one obtained at point C in Fig. 4a.

Curiously enough, the neutral factor k_N takes negative values for A6 when using ML criterion (Fig. 4b), this meaning that the connection of the neutral reduces the maximum achievable torque. However, a high price in terms of torque/current production is to be paid when using the ML, being 28.2/64.3% lower compared to the MT criterion in 1N (point A in Fig. 4c). In general, k_M is always positive, i.e. ML criterion increases the derating of drive. Considering that i) the post-fault torque capability is already limited by the fault occurrence and ii) efficiency is not a main concern in post-fault situation, the MT criterion seems in principle a better choice. Since the aim of this paper is to explore the limits of torque capability in fault-tolerant six-phase drives, the subsequent results will focus exclusively on MT criterion.

As far as the scenario 1 is concerned, some conclusions can be inferred:

- D3 is the worst option from the fault tolerance point of view.
- A6 provides the best post-fault capability in 2N.
- The use of 1N highly elevates the post-fault torque production.
- ML criterion significantly reduces the maximum achievable torque compared to MT, as expected.
- S6 is the best choice in 1N, and the maximum current and torque production using MT is 77.1 and 59.4%, respectively.

B. Two OCFs (scenarios 2a, 2b, 2c, 2d)

The scenarios with two OCFs are examined next. Figs. 5a-5b show the derating factor a for 2N and 1N, respectively, and Fig. 5c presents the neutral factor k_N . Similar to 1 OCFs, the connection of the neutrals does not improve the performance for D3, but a somewhat higher value of the derating factor a is obtained with A6 and S6 (55.7 and 57.7%, respectively in case 2a with 1N). The improvement from 2N to 1N is however less pronounced than in scenario 1, obtaining a neutral factor k_N below 20% in the whole range of γ . In scenario 2b the derating is the same regardless of the neutral connection ($k_N = 0$), and again S6 is the best choice in terms of fault tolerance. In fact D3 is not fault-tolerant at all in scenario 2b, whereas A6 and S6 increase the current capability up to 29 and 50%, respectively. Scenario 2c shows however a significant difference between 1N and 2N. While in 1N the best machine is again S6, in 2N the best machine is D3, A6 has

low fault-tolerant capability and S6 has no fault tolerance, this causing a dramatic increase of the neutral factor k_N with increasing values of γ . Finally, scenario 2d shows no difference between 1N and 2N, this being similar to scenario 2b. Nevertheless, in this case the best choice is the A6 compared to D3 and S6.

It is worth noting that unlike 1 OCFs, 2 OCFs can lead to single-phase operation which renders some of the machine useless (hence $a = 0$). In this regard, D3 is the worst, where scenario 2b is fatal for both D3-1N and D3-2N. S6 is slightly better, with only S6-2N susceptible to single-phase operation under scenario 2c. Overall, A6 is the most robust and is resilient to all 2 OCFs.

Some additional conclusions can be extracted from the analysis of the scenarios with 2 OCFs:

- The performance improvement obtained with the connection of the neutrals is low. 1N is only clearly better than 2N in one out of four scenarios.
- In 2N the fault-tolerant performance of the three mainstream six-phase machines is similar.
- In 1N the performance of S6 is globally the best, but the A6 presents a comparable performance in three out of four scenarios.
- A6 is resilient against all 2 OCFs and is the best choice in terms of overall fault tolerance.

C. Three OCFs (scenarios 3a, 3b, 3c, 3d)

To conclude the analysis, the derating under three OCFs is finally examined in Fig. 6. It must be noted that in these scenarios the post-fault operation in 2N is only feasible for scenario 2a, where the three OCFs occur in the VSC₁ and the solution is consequently trivial and equal to the ‘single VSC’ mode of operation that provides 50% of the current production. In all other scenarios, windings $a_1b_1c_1$ are disabled by two OCFs while the remaining OCF reduces windings $a_2b_2c_2$ to single-phase system which creates a pulsating (non-circular) MMF. The additional degree of freedom added in 1N makes it possible to operate in scenarios 3b, 3c and 3d, but with a low fault tolerant capability for all values of γ . D3 has no fault tolerance in scenarios 3b and 3d. A6 and S6 have some fault-tolerance in all scenarios with three OCFs, but obtaining low torque/power. If the aim is to allow at least some post-fault

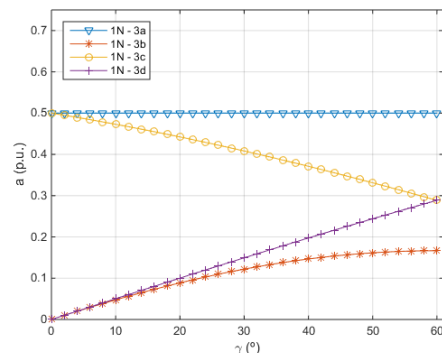


Fig. 6: Derating factor a versus spatial shifting angle γ for 3 OCFs (scenarios 3a, 3b, 3c and 3d) in single neutral (1N) configuration.

operations in all possible scenarios, then S6 would be the best choice but the general conclusion is that the fault tolerant capability is mostly inexistent for 2N and low for 1N.

D. Summary

In order to somehow gather the results from Fig. 4-6 and extract global conclusions, Table II summarizes the best (B), worst (W) and medium-choice (M) among the three mainstream machines (D3, A6 and S6) for 1N and 2N and all possible scenarios. The information is completed with a background color according to the following thresholds:

- Blue (↑) → current > 70% torque > 49%
- Green (↑) → current > 50% torque > 25%
- Orange (↓) → current > 33% torque > 11%
- Grey (↓) → current < 33% torque < 11%

Even though there is not a simple trend, it can be globally concluded that the S6 is the best six-phase machine when in 1N whereas A6 is the best choice in 2N. It can also be inferred that the 1N provides better performance in two aspects: *i*) it can withstand a wider range of faults and still obtain some fault tolerance, and *ii*) it provides the highest post-fault current/torque for S6 in scenario 1, which is the most likely to occur in practice.

As general rules for the selection of a six-phase machine, the following situations would benefit the selection of D3, A6 and S6:

- D3-2N can be selected if the fault tolerance is not a relevant issue and other features (simplicity, dc-bus utilization, no excitation *x-y* currents) are promoted instead. D3-1N is not a good option in any case.
- A6-2N can be selected to improve the fault-tolerant capability of D3 and still maintain simplicity and better dc-bus utilization. It also has the best fault-tolerance if up to 2 OCFs are anticipated.
- S6-1N is the best choice if fault tolerance is a main concern.

TABLE II
BEST, MEDIUM-CHOICE AND WORST PERFORMANCE OF SIX-PHASE MACHINES ACCORDING TO THEIR FAULT-TOLERANT CAPABILITY

NC	FS	S6	A6	D3	NC	FS	S6	A6	D3
1N	1	B ↑	M ↑	W ↓	2N	1	M ↓	B ↑	M ↓
	2a	B ↑	M ↑	W ↓		2a	M ↓	M ↓	M ↓
	2b	B ↓	M ↓	W ↓		2b	B ↓	M ↓	W ↓
	2c	B ↑	M ↓	W ↓		2c	W ↓	M ↓	B ↓
	2d	M ↓	B ↑	M ↓		2d	M ↓	B ↑	M ↓
	3a	M ↓	M ↓	M ↓		3a	M ↓	M ↓	M ↓
	3b	B ↓	M ↓	W ↓		3b	-	-	-
	3c	W ↓	M ↓	B ↓		3c	-	-	-
	3d	B ↓	M ↓	W ↓		3d	-	-	-

TABLE III
RECONFIGURATION OF X-Y AND 0-0. REFERENCE CURRENTS IN POST-FAULT SITUATION FOR ALL INDEPENDENT SCENARIOS IN 1N AND 2N

Fault	1N									2N				
	K ₁	K ₂	K ₃	K ₄	K ₅	K ₆	K ₇	K ₈	a	K ₁	K ₂	K ₃	K ₄	a
A6														
1	-0.641	-0.209	-0.754	-0.296	-0.359	0.209	0.359	-0.209	0.694	-1	0	0	-1	0.577
2a	-0.536	0.268	-0.804	0.536	-0.464	-0.268	0.464	0.268	0.558	-1	0	0	1	0.500
2b	-1	0	-3.464	-1	0	0	0	0	0.289	-1	0	-3.464	-1	0.289
2c	0	-0.268	-0.268	0	-1	0.268	1	-0.268	0.558	-1	0	3.464	-1	0.289
2d	-1	0	0	-1	0	0	0	0	0.577	-1	0	0	-1	0.577
3a	-1	0	0	1	0	0	0	0	0.500	-1	0	0	1	0.500
3b	1.366	1.366	-4.097	-1.366	-2.365	-1.366	2.365	1.366	0.122	-	-	-	-	0
3c	-1	0.732	0	-0.268	0	-0.732	0	0.732	0.408	-	-	-	-	0
3d	0.732	-1	-3	2.732	-1.732	1	1.732	-1	0.149	-	-	-	-	0
S6														
1	-0.648	0	0	-0.368	-0.352	0	0.352	0	0.771	-1	0	0	-0.3334	0.500
2a	-0.750	0.433	-0.433	0.250	-0.250	-0.433	0.250	0.433	0.577	-1	0	0	1	0.500
2b	-1	0	-1.155	-1	0	0	0	0	0.500	-1	0	-1.155	-1	0.500
2c	0	0	0	0	-1	0	1	0	0.577	-	-	-	-	0
3a	-1	0	0	1	0	0	0	0	0.500	-1	0	0	1	0.500
3b	0	1.732	-1.732	-2	-1	-1.732	1	1.732	0.167	-	-	-	-	0
3c	-1.500	0.866	0.866	-0.500	0.500	-0.866	-0.500	0.866	0.289	-	-	-	-	0
D3														
1	-0.667	0.577	1.732	0	-0.333	-0.577	0.333	0.577	0.500	-1	0	0	-0.3334	0.500
2a	-0.333	0	-1.155	1	-0.667	0	0.667	0	0.500	-1	0	0	1	0.500
3a	-1	0	0	1	0	0	0	0	0.500	-1	0	0	1	0.500

The results presented here are based on the assumption that the machines have distributed windings, and the effect of both zero sequence and x - y subspaces under different fault scenarios can, to large extent, be neglected. Furthermore, the dc-link voltage is assumed to be sufficiently high for the controller to operate in post-fault operation without going into the overmodulation region [35].

IV. FAULT-TOLERANT CONTROL

Following the VSD optimization approach described in section II it is possible to determine the relationship between x - y - 0_+ and α - β currents for the three mainstream machines in all possible scenarios and neutral arrangements (see Table III). It is however necessary to include this information into a suitable fault-tolerant control scheme in order to smoothly drive the six-phase machine after the fault occurrence. The standard indirect rotor-flux field oriented control (IRFOC) [1] can be applied in post-fault situation to generate the α - β reference voltages, but the regulation of the x - y plane requires to main changes: *i*) it is necessary to switch for null pre-fault values to those shown in Table III and *ii*) it is necessary to use proportional-resonant (PR) controllers, or equivalent dual-PI regulators in synchronous and anti-synchronous references frames using the park transformation D (Fig. 6). The use of PR controllers allows tracking ac x - y reference currents with good performance [10,17-18]. The modified x - y current loop provides x - y reference voltages that, together with the α - β reference voltages from the IRFOC are transformed into phase values for the modulation stage that finally provides the switching signals to the VSCs. Apart from the number of dual PI regulators (i.e. one less in 2N case), the control scheme remains the same regardless of the six-phase machine (D3, A6 or S6) and neutral connection.

V. EXPERIMENTAL RESULTS

A. Test rigs.

The experimental results are obtained using two test rigs, one for the A6 machine (test rig 1) and another one for the S6/D3 machine (test rig 2). The A6 (S6/D3) machine is obtained by rewinding a 1.2 kW (1.1 kW) three-phase induction machine. The general layout for both test rigs is shown in Fig. 7. In test rig 1 (test rig 2), the A6-IM (S6/D3-IM) is driven by two three-phase two level voltage source converters based on Semikron SKS22F modules (SKM75GB12T4 modules) that correspond to VSC₁ and VSC₂ in Fig. 7. The converters are connected to a DC power supply system and the control is implemented via Texas Instrument TMS320F28335 Digital Signal Controller (dSpace DS1103 rapid prototyping system). Current and speed measurements are taken with LEM LAH 25-NP (LEM LTSR-15-NP) hall-effect sensors and GHM510296R/2500 (E60H20-5000-3-N-5) digital encoder, respectively. The load torque is provided by a DC generator (permanent magnet generator) connected to a variable resistive-inductive load. OCFs are created by physically

disconnecting the inverter from between the motor phases using relays.

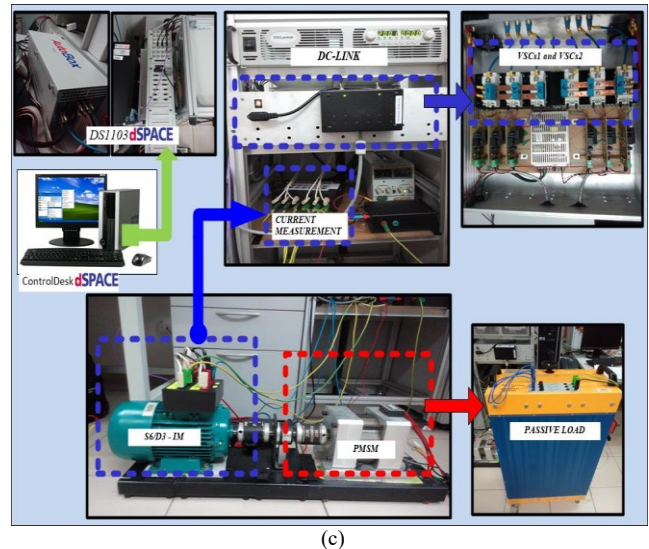
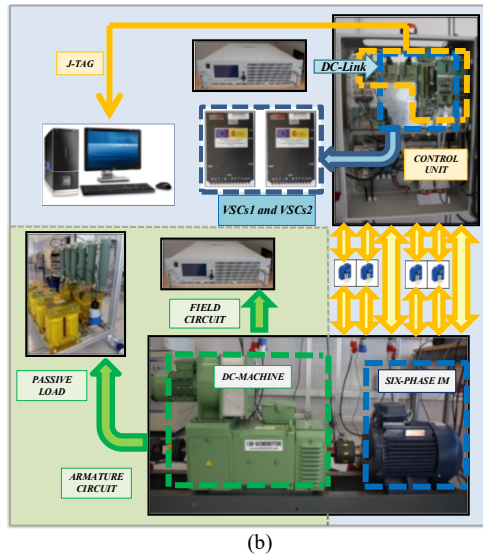
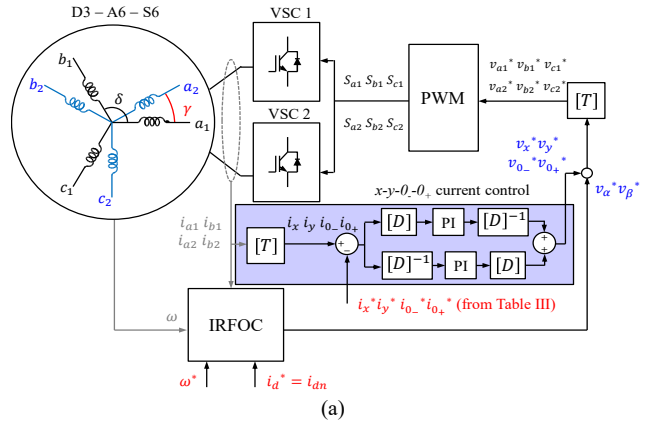


Fig. 7: Prototype machine and experimental setup (a) Fault-tolerant control scheme with PR (dual PI) controllers in the x - y current loop (b) Test-rig A6-IM (c) Test-rig S6/D3-IM.

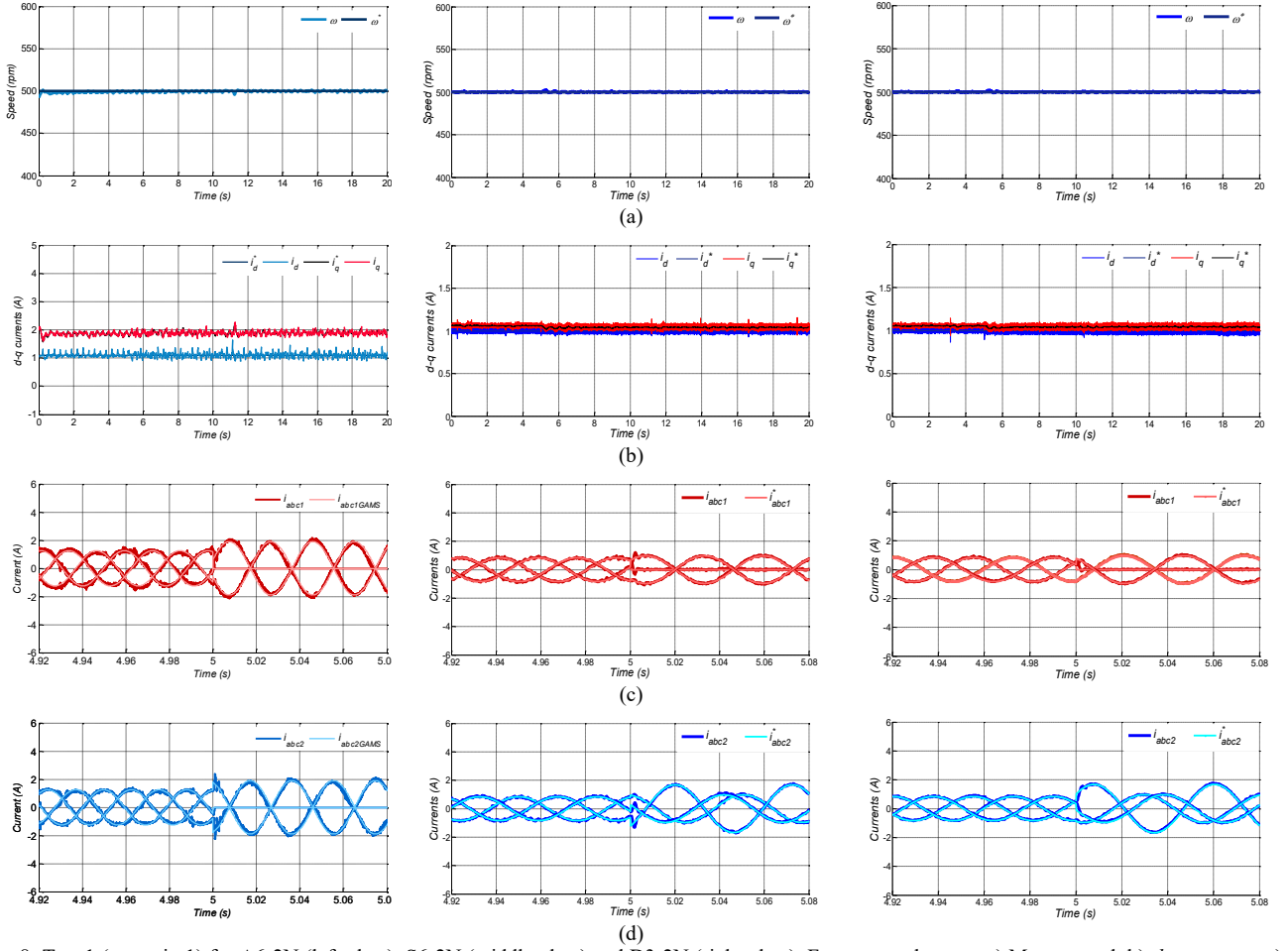


Fig. 8: Test 1 (scenario 1) for A6-2N (left plots), S6-2N (middle plots) and D3-2N (right plots). From top to bottom: a) Motor speed, b) d - q currents, c) phase currents of winding 1 and d) phase currents of winding 2.

B. Experimental results

Since the number of independent tests to cover all possible scenarios and neutral arrangements is high, the following subset is selected as representative of the post-fault performance in the event of 1, 2 or 3 OCFs: test 1 covers scenario 1 for 2N, test 2 covers scenario 2a for 1N and test 3 covers scenario 3a for 1N. Other scenarios have also been tested but are omitted here for the sake of brevity.

Results from test 1, test 2 and test 3 are shown in Fig. 8, Fig. 9 and Fig. 10 respectively. In all cases, the speed (subplot (a) in Figs. 8-10) is maintained in pre- ($t < 5$ s) and post- ($t > 5$ s) fault situations. This is achieved because the d - q currents maintain the same value before and after the fault (subplot (b) in Figs. 8-10). On the contrary, x - y and θ_+ - θ_- current references need to be changed from zero (pre-fault) to the values shown in Table III (post-fault). The dual PI controller shown in Fig. 7a is in charge of tracking these non-zero components.

The injection of the secondary currents in turn modifies the phase currents according to the MT criterion. Subplots (c) and (d) show the measured phase currents for windings 1 (dark red trace) and 2 (dark blue trace) together with the optimal currents for windings 1 (light red trace) and 2 (light

blue trace) calculated with software (GAMS and Solver) according to the optimization procedure. Generally, the current tracking is satisfactory both in pre- and post-fault situations for all cases.

It must be noted that the α - β current derating in 2N for A6 (0.577 p.u.) is obtained considering the same phase current limits before and after the fault (Fig. 4). On the contrary, the α - β current (reflected as d - q currents) is the same in Fig. 8-10 and consequently the phase currents are increased accordingly in post-fault situation.

For test 1, the speed and d - q currents are essentially the same before and after fault, confirming the validity of the post-fault control. As expected, the phase currents increase after fault, with the pre-fault current being 0.577, 0.5 and 0.5 times the maximum post-fault currents for A6, S6 and D3, respectively, in accordance with their respective derating factor in Table III.

The results for tests 2 and test 3 for A6, S6 and D3 are shown next in Figs. 9-10. As in test 1, the speed is maintained and consequently d - q currents are also maintained before and after the fault occurrence (subplot (b) in Figs. 9-10). For test 2, the increase of phase current after fault is the highest for D3 (derating factor, $a = 0.5$),

followed by A6 ($a = 0.558$) and S6 ($a = 0.577$). Again a good match between the reference currents (based on Table III) and actual post-fault current were obtained.

Though omitted for brevity in Figs. 8-10, x - y and θ_+ - θ_- current references are obtained from table III and the dual PI controller shown in Fig. 7a allows a satisfactory tracking of the secondary components.

VI. CONCLUSIONS

Quantification of the post-fault capability to generate current/torque is relevant to identify the degree of fault-tolerance, the most suitable choice for the winding displacement and neutral arrangement in six-phase motors. This contribution provides a full picture of the derating under different types of machines, neutral configurations and fault scenarios. Even though the performance depends on the conditions of each specific case, the unified analysis allows extracting some general conclusions:

- ✓ **Type of six-phase machine (D3/A6/S6):** S6 is globally the machine with a higher post-fault capability in 1N, achieving a maximum post-fault current of 77.1% under 1 OCF and $\geq 50\%$ for all 2

OCFs scenarios. A6 is in turn the best choice in 2N, although the performance is quite similar to S6. Even though D3 has better performance than A6 and S6 in some specific scenarios, it is by and large the worst choice in terms of fault tolerance.

- ✓ **Type of neutral connection (1N/2N):** 1N provides better fault-tolerant capability than 2N in all scenarios. The improvement is relevant under 1 OCF scenario, minor with 2 OCFs and allows operating in all scenarios with 3 OCFs (except for D3).
- ✓ **Type of fault scenario (1/2/3 OCFs):** the scenario with 1 OCF clearly promotes the use of S6-1N. For 2 OCFs A6-1N and S6-1N have very similar performance. However, in terms of 2N connection, A6-2N is the best by being tolerant to all 2 OCFs. In scenarios with 3 OCFs the post-fault operation is unfeasible in 2N (except case 3a) and provides only marginal current/torque in 1N.

As far as the fault tolerance is concerned, the aforementioned conclusions serve as guidelines for the selection of the most suitable six-phase machine for each specific application.

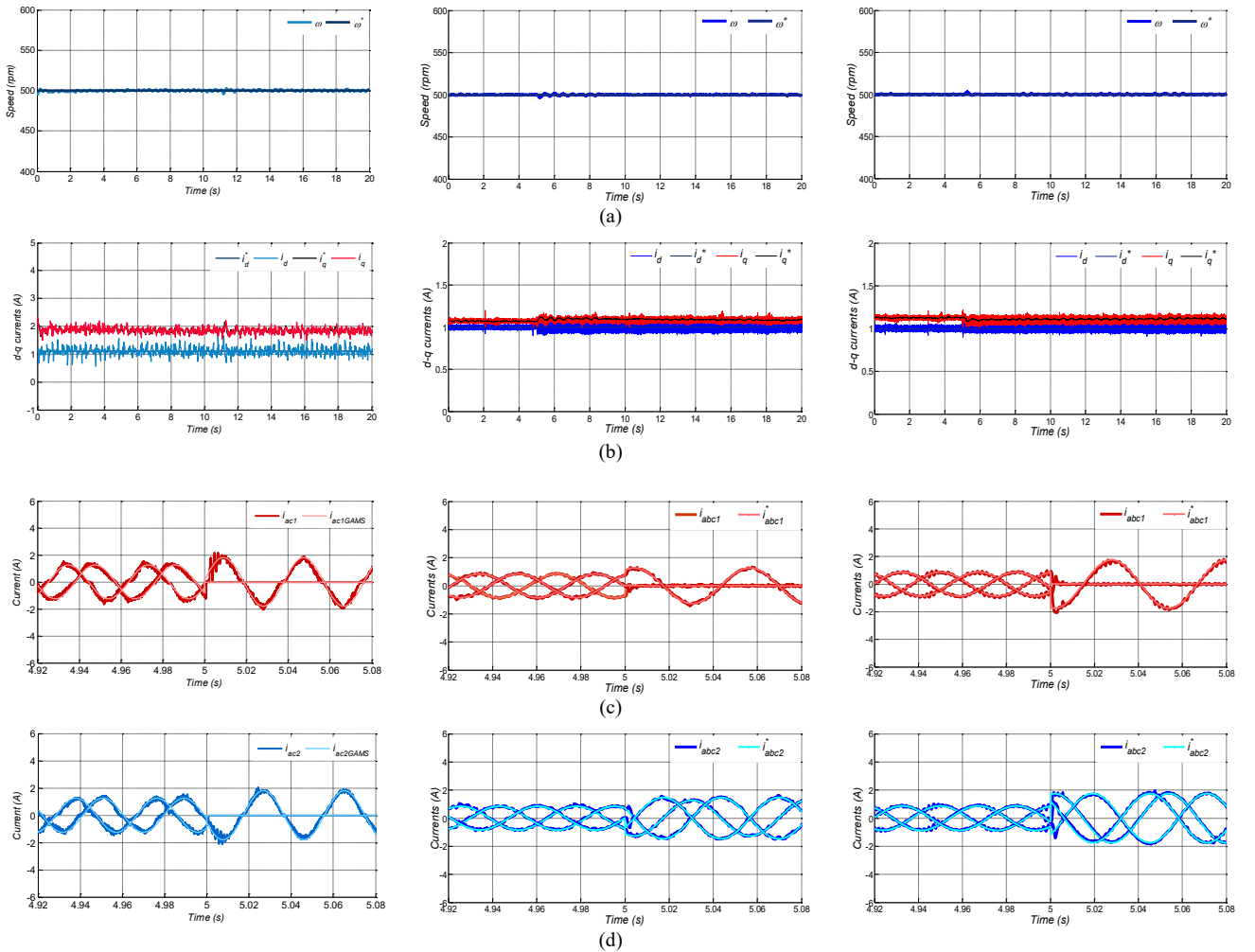


Fig. 9: Test 2 (scenario 2a) for A6-1N (left plots), S6-1N (middle plots) and D3-1N (right plots). From top to bottom: a) Motor speed, b) d - q currents, c) phase currents of winding 1 and d) phase currents of winding 2..

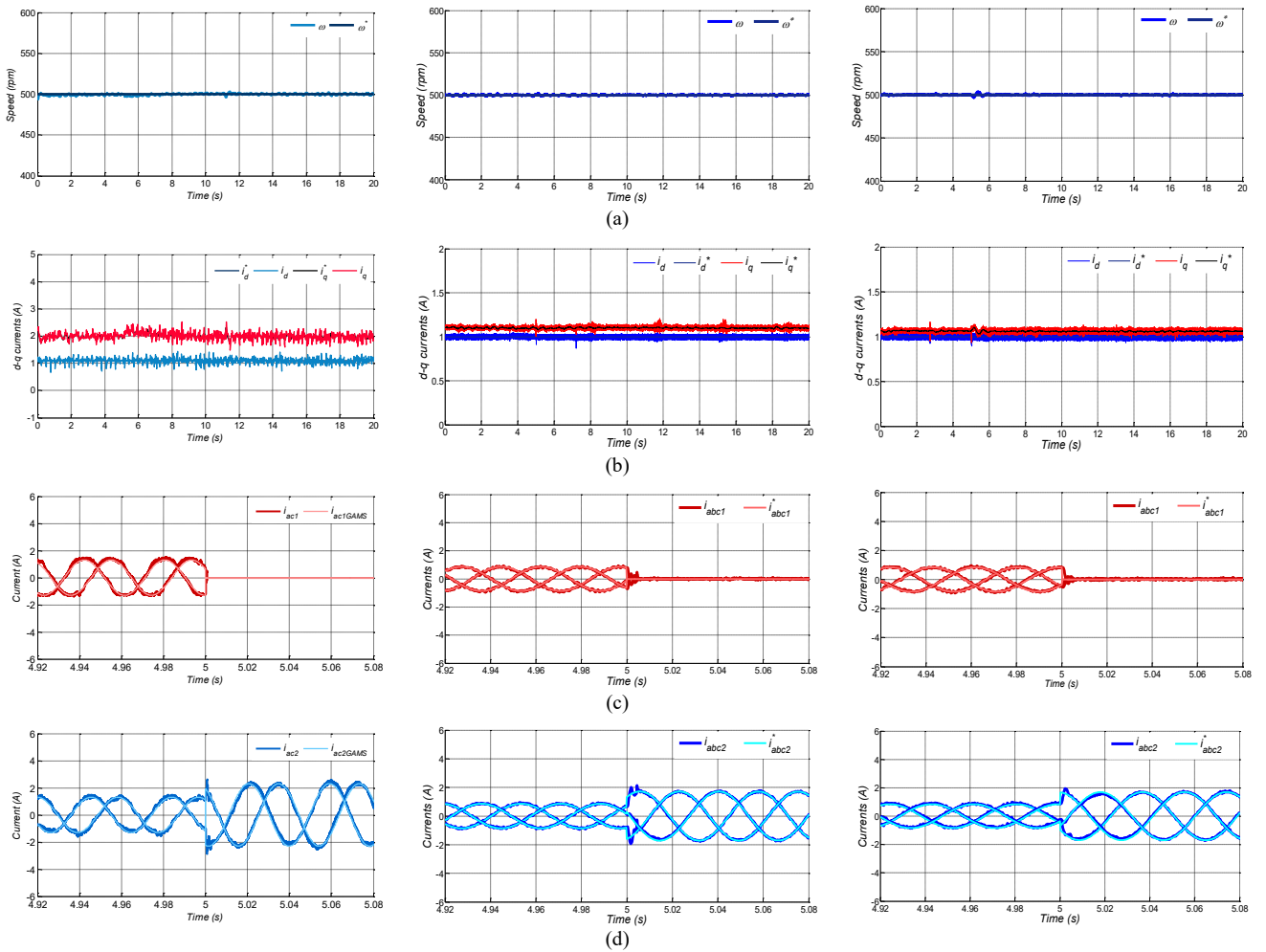
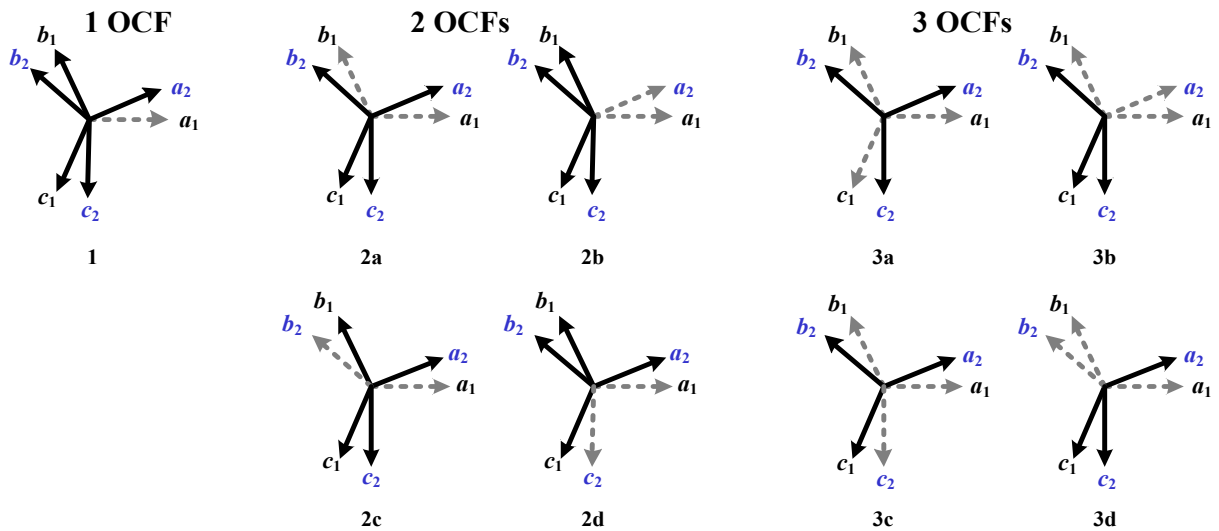


Fig. 10: Test 3 (scenario 3a) for A6-1N (left plots), S6-1N (middle plots) and D3-1N (right plots). From top to bottom: a) Motor speed, b) d - q currents, c) phase currents of winding 1 and d) phase currents of winding 2.

APPENDIX: STATOR WINDING CONNECTIONS UNDER DIFFERENT FAULT SCENARIOS



Note: Dotted line indicates open-circuited phase winding.

ACKNOWLEDGEMENT

The authors would like to acknowledge the support from the Malaysian government through the Fundamental Research Grant Scheme (FP049-2014B), University of Malaya Research Grant (RG296-14AFR) and Higher Institution Centre of Excellence (HICoE) Program Research Grant, UMPEDAC - 2016 (MOHE HICoE - UMPEDAC), as well as the Spanish Ministry of Science and Innovation via Project ENE2014-52536-C2-1-R.

REFERENCES

- [1] E. Levi, R. Bojoi, F. Profumo, H.A. Toliyat and S. Williamson, "Multiphase induction motor drives - A technology status review," *IET Electric Power Applications*, vol. 1, no. 4, pp. 489-516, 2007.
- [2] E. Levi, F. Barrero and M.J. Duran, "Multiphase machines and drives - Revisited," *IEEE Trans. Ind. Electron.*, vol. 63, no. 1, pp. 429-432, 2016.
- [3] E. Levi, "Advances in converter control and innovative exploitation of additional degrees of freedom for multiphase machines," *IEEE Trans. Ind. Electron.*, vol. 63, no. 1, pp. 433-448, 2016.
- [4] F. Barrero and M.J. Duran, "Recent advances in the design, modeling and control of multiphase machines - Part 1," *IEEE Trans. Ind. Electron.*, vol. 63, no. 1, pp. 449-458, 2016.
- [5] M.J. Duran and F. Barrero, "Recent advances in the design, modeling and control of multiphase machines - Part 2," *IEEE Trans. Ind. Electron.*, vol. 63, no. 1, pp. 459-468, 2016.
- [6] H.S. Che, E. Levi, M. Jones, M.J. Duran, W.P. Hew, and N.A. Rahim, "Operation of a six-phase induction machine using series-connected machine-side converters," *IEEE Trans. Ind. Electron.*, vol. 61, no. 1, pp. 164-176, 2014.
- [7] I. Subotic, N. Bodo, E. Levi and M. Jones, "Onboard integrated battery charger for EVs using an asymmetrical nine-Phase Machine," *IEEE Trans. Ind. Electron.*, vol. 62, no. 5, pp. 3285-3295, 2015.
- [8] H. Guzman, M.J. Duran, F. Barrero, B. Bogado and S. Toral, "Speed control of five-phase induction motors with integrated open-phase fault operation using model-based predictive current control techniques," *IEEE Trans. Ind. Electron.*, vol. 61, no. 9, pp. 4474-4484, 2014.
- [9] H. Guzman, F. Barrero and M.J. Duran, "IGBT-gating failure effect on a fault-tolerant predictive current controlled 5-phase induction motor drive," *IEEE Trans. on Industrial Electronics*, vol. 62, no. 1, pp. 15-20, 2015.
- [10] H. Guzman, M.J. Duran, F. Barrero, B. Bogado, I. Gonzalez-Prieto and M.R. Arahal, "Comparative study of predictive and resonant controllers in fault-tolerant five-phase induction motor drives," *IEEE Trans. Ind. Electron.*, vol. 63, no. 1, pp. 606-617, 2016.
- [11] "Gamesa 5.0 MW" Gamesa Technological Corporation S.A., 2016. Online available: <http://www.gamesacorp.com/recursos/doc/productos-servicios/aerogeneradores/catalogo-g10x-45mw.pdf>
- [12] C. Dittmanson, P. Hein, S. Kolb, J. Mólck and S. Bernet, "A new nodular flux-switching permanent-magnet drive for large wind turbines," *IEEE Ind. Appl. Mag.*, vol. 50, no. 6, pp. 3787-3794, 2014.
- [13] E. Jung, H. Yoo, S. Sul, H. Choi and Y. Choi, "A nine-phase permanent-magnet motor drive system for an ultrahigh-speed elevator," *IEEE Trans. Ind. Appl.*, vol. 48, no. 3, pp. 987-995, 2012.
- [14] W. Cao, B.C. Mecrow, G.J. Atkinson, J.W. Bennett and D.J. Atkinson, "Overview of electric motor technologies used for more electric aircraft (MEA)" *IEEE Trans. on Ind. Electron.*, vol. 59, no. 9, pp. 3523-3531, 2012.
- [15] J. Wang; Y. Li and Y. Han, "Integrated modular motor drive design with GaN power FETs," *IEEE Trans. on Ind. Appl.*, vol. 51, no. 4, pp. 3198-3207, 2015.
- [16] S.S. Gjerde, P.K. Olsen, K. Ljokelsoy and T.M. Undeland, "Control and fault handling in a modular series-connected converter for a transformerless 100 kV low-weight offshore wind turbine," *IEEE Trans. Ind. Appl.*, vol. 50, no. 2, pp. 1094-1105, 2014.
- [17] H.S. Che, M.J. Duran, E. Levi, M. Jones, W.P. Hew and N.A. Rahim, "Post-fault operation of an asymmetrical six-phase induction machine with single and two isolated neutral points," *IEEE Trans. Power Electron.*, vol. 29, no. 10, pp. 5406-5416, 2014.
- [18] M.J. Duran, I. Gonzalez-Prieto, M. Bermudez, F. Barrero, H. Guzman and M.R. Arahal, "Optimal fault-tolerant control of six-phase induction motor drives with parallel converters" *IEEE Trans. Ind. Electron.*, vol. 63, no. 1, pp. 629-640, 2016.
- [19] A. E. Ginart, P. W. Kalgren, M. J. Roemer, D. W. Brown, and M. Abbas, "Transistor diagnostic strategies and extended operation under one-transistor trigger suppression in inverter power drives," *IEEE Trans. Power Electron.*, vol. 25, no. 2, pp. 499-506, 2010.
- [20] A. Tani, M. Mengoni, L. Zarri, G. Serra, and D. Casadei, "Control of Multiphase Induction Motors With an Odd Number of Phases Under Open-Circuit Phase Faults," *IEEE Trans. Power Electron.*, vol. 27, no. 2, pp. 565-577, 2012.
- [21] H. Ryu, J. Kim, and S. Sul, "Synchronous-Frame Current Control of Multiphase Synchronous Motor Under Asymmetric Fault Condition Due to Open Phases," *IEEE Trans. Ind. Appl.*, vol. 42, no. 4, pp. 1062-1070, 2006.
- [22] R. H. Nelson and P. C. Krause, "Induction machine analysis for arbitrary displacement between multiple winding sets," *IEEE Trans. Power Appar. Syst.*, vol. PAS-93, no. 3, pp. 841-848, 1974.
- [23] D. Dujic, A. Iqbal, and E. Levi, "A space vector PWM technique for symmetrical six-phase voltage source inverters," *EPE J.*, vol. 17, no. 1, pp. 24-32, 2007.
- [24] H.S. Che and W.P. Hew, "Dual three-phase operation of single neutral symmetrical six-phase machine for improved performance," in proc. of *IECON 2015 - 41st Annual Conference of the IEEE*, pp. 001176 - 001181, 2015.
- [25] G. Zhang, W. Hua, M. Cheng and J. Liao, "Design and comparison of two six-phase hybrid-excited flux-switching machines for EV/HEV applications," *IEEE Trans. Ind. Electron.*, vol. 63, no. 1, pp. 481-493, 2016.
- [26] A. Cavagnino, Z. Li, A. Tenconi and S. Vaschetto, "Integrated generator for more electric engine: design and testing of a scaled-size prototype," *IEEE Trans. Ind. Appl.*, vol. 49, no. 5, pp. 2034-2043, 2013.
- [27] X. Huang, A. Googman, C. Gerada, Y. Fang and Q. Lu, "Design of a five-phase brushless DC motor for a safety critical aerospace application," *IEEE Trans. Ind. Electron.*, vol. 59, no. 9, pp. 3532-3541, 2012.
- [28] X. Xue, W. Zhao, J. Zhu, G. Liu, X. Zhu and M. Cheng, "Design of five-phase modular flux-switching permanent-magnet machines for high reliability applications," *IEEE Trans. Magn.*, vol. 49, no. 7, pp. 3941-3944, 2013.
- [29] A. S. Abdel-Khalik, M. A. Elgenedy, S. Ahmed, and A.M. Massoud, "An improved fault-tolerant five-phase induction machine using a combined star/pentagon single layer stator winding connection," *IEEE Trans. Ind. Electron.*, vol. 63, no. 1, pp. 618-628, 2016.
- [30] A. Pantea, A. Yazidi, F. Betin, M. Taherzadeh, S. Carriere, H. Henaou, G. Capolino, "Six-phase induction machine model for electrical fault simulation using the circuit-oriented method," *IEEE Trans. Ind. Electron.*, vol. 63, no. 1, pp. 494-503, 2016.
- [31] L. Shao, W. Hua, N. Dai, M. Tong, and M. Cheng, "Mathematical modeling of a 12-phase flux-switching permanent-magnet machine for wind power generation," *IEEE Trans. Ind. Electron.*, vol. 63, no. 1, pp. 504-516, 2016.
- [32] R. Bojoi, A. Cavagnino, A. Tenconi, and S. Vaschetto, "Control of shaftline-embedded multiphase starter/generator for aero-engine," *IEEE Trans. Ind. Electron.*, vol. 63, no. 1, pp. 641-652, 2016.
- [33] I. Gonzalez-Prieto, M.J. Duran, H.S. Che, E. Levi, M. Bermudez and F. Barrero "Fault-tolerant Operation of Six-phase Energy Conversion Systems with Parallel Machine-side Converters," *IEEE Trans. Power Electron.*, vol. 31, no. 4, pp. 3068-3079, 2016.
- [34] I. Gonzalez-Prieto, M.J. Duran, F. Barrero, M. Bermudez and H. Guzman, "Impact of post-fault flux adaptation on six-phase induction motor drives with parallel converters," *IEEE Trans. Power Electron.*, early access, 2016.
- [35] A.S. Abdel-Khalik, M.I. Masoud, S. Ahmed and A. Massoud, "Calculation of derating factors based on steady-state unbalanced multiphase induction machine model under open phase(s) and optimal winding currents," *Electric Power System Research*, vol. 106, pp. 214-225, 2014.
- [36] N. Bianchi, E. Fornasiero and S. Bolognani, "Thermal analysis of a five-phase motor under faulty operations," *IEEE Trans. Ind. Appl.*, vol. 49, no. 4, pp. 1531-1538, 2013.
- [37] GAMS web, "A User's Guide", Available: <http://gams.com/doc>



Wan Noraishah Wan Abdul Munim received the Diploma in Electrical Engineering (Telecommunication) from University Teknologi Malaysia (UTM), Malaysia in 2003. She received the B.Eng. Technology degree in electrical engineering from Universiti Kuala Lumpur (UniKL), Malaysia in 2007 and M.Sc. in Electrical Power Engineering with Business from the University of Strathclyde, Glasgow, U.K. in 2009.

She has been a lecturer with Universiti Teknologi MARA (UiTM), Malaysia since 2010 and is currently working toward her PhD degree at UMPEDAC, University of Malaya, Malaysia. Her research interests include multiphase machines, fault tolerant control, and renewable energy.

She received the 2014 Ministry of Education Malaysia Skim Latihan Akademik IPTA (SLAI) Scholarship Award for her PhD study.



Nasrudin Abd Rahim (M'89–SM'08) received the B.Sc. (Hons.) and M.Sc. degrees from the University of Strathclyde, Glasgow, U.K., and the Ph.D. degree from Heriot–Watt University, Edinburgh, U.K., in 1995. He is currently a Professor with the University of Malaya, Kuala Lumpur, Malaysia, where he is also the Director of the UM Power Energy Dedicated Advanced Centre (UMPEDAC). He is also a Distinguish Adjunct Professor at Renewable Energy Research Group, King

Abdulaziz University, Jeddah, Saudi Arabia. His research interests include power electronics, Solar PV and wind technologies, realtime control systems, and electrical drives. Prof. N A Rahim is a fellow of the Institution of Engineering and Technology, U.K., the Academy of Sciences Malaysia and Senior Member IEEE. He is also a Chartered Engineer (U.K.).



Mario J. Duran was born in Málaga, Spain, in 1975. He received the M.Sc. and Ph.D. degrees in Electrical Engineering from the University of Málaga Spain, in 1999 and 2003, respectively.

He is currently an Associate Professor with the Department of Electrical Engineering at the University of Málaga. His research interests include modeling and control of multiphase drives and renewable energies conversion systems.



Hang Seng Che received his BEng degree in Electrical Engineering from the University of Malaya (Kuala Lumpur, Malaysia) in 2009, before completing his PhD degree in 2013 under auspices of a dual PhD programme between the University of Malaya and Liverpool John Moores University (Liverpool, UK).

Since 2013, he has been with UMPEDAC, University of Malaya, where he currently serves as Senior Lecturer. He is an Associate Editor for

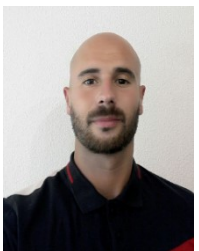
IET Electric Power Applications (IET-EPA) journal since 2016.

Dr. Che was the recipient of the 2009 Kuok Foundation Postgraduate Scholarship Award for his PhD study. His research interests include multiphase machines and drives, fault tolerant control, and power electronics converters for renewable energy applications.



Mario Bermudez was born in Málaga, Spain, in 1987. He received the Industrial Engineer degree from the University of Málaga, Málaga, Spain, in 2014. He is currently working toward the Ph.D. degree in the Laboratory of Electrical Engineering and Power Electronics of Lille (L2EP), Arts et Métiers ParisTech, Lille, France, and in the Department of Electronic Engineering, University of Seville, Seville, Spain.

His research interests include modeling and control of multiphase drives, DSP-based systems and electrical vehicles.



Ignacio Gonzalez Prieto was born in Malaga, Spain, in 1987. He received the Industrial Engineer and M. Sc. degrees from the University of Malaga, Spain, in 2012 and 2013, respectively. He obtained the PhD degree in Electronic Engineering from the University of Seville, Spain, in 2016.

His research interests include multiphase machines, wind energy systems and electrical vehicles.